Chiral tunneling through a time-periodic potential in monolayer graphene

M. Ahsan Zeb
National Centre for Physics, Islamabad 45320, Pakistan
and Department of Physics, Quaid-i-Azam University, Islamabad 45320, Pakistan

K. Sabeeh*
Department of Physics, Quaid-i-Azam University, Islamabad 45320, Pakistan

M. Tahir
Department of Physics, University of Sargodha, Sargodha 40100, Pakistan

(Received 12 April 2008; revised manuscript received 25 July 2008; published 24 October 2008)

Chiral tunneling through a harmonically driven potential barrier in a graphene monolayer is considered in this work. Since the charge carriers in this system are massless, chiral Dirac particles, tunneling is described as Klein tunneling and is highly anisotropic. To study Klein tunneling through a harmonically driven potential barrier, we determine the transmission probabilities for the central band and sidebands as the incident angle of the electron beam is changed. Furthermore, we investigate the transmission probabilities as the width, amplitude, and frequency of the oscillating barrier are changed. Interestingly, perfect transmission for normal incidence that has been reported for a static barrier persists for the oscillating barrier which is a manifestation of Klein tunneling in a time-harmonic potential.

DOI: 10.1103/PhysRevB.78.165420 PACS number(s): 72.80.Rj

I. INTRODUCTION

Advancement in technology has led to active investigation of electron transport in semiconductor nanostructures in time-dependent fields. The additional degree of freedom provided by time dependence has led to the appearance of new phenomena in electron transport; for a review, see Ref. 1 and references therein. Engineering of confinement potential and band structure has allowed the possibility of studying photon-assisted tunneling (PAT), where inelastic tunneling events occur in the presence of an ac field, in various driven systems. This topic is not only of academic interest but also has device applications. Early studies of PAT include the work of Dayem and Martin[2] that provided evidence of absorption and emission of photons in tunneling transport in experiments on superconducting films in the presence of microwave fields. Soon after this, Tien and Gordon[3] theoretically justified this observation. They assumed a time-harmonic potential difference produced between the two films by a microwave field and solved the time-dependent Schrödinger equation for the system. Their photon-assisted transport model accounted for transmission in sidebands in the presence of microwave radiation. The basic physical idea behind photon-assisted tunneling is that an oscillating potential can lead to inelastic tunneling where the electrons exchange energy quanta (photons) with the oscillating field. In these systems, a harmonically time-driven potential results in exchange of energy with electrons in the units of modulation quanta $\hbar\omega$, with ω being the modulation frequency. Therefore, electrons at energy E can be transferred to sidebands at energies $E \pm n\hbar\omega$ $(n=0, \pm 1, \pm 2, \ldots)$ while traversing a region of space subjected to such a time-harmonic potential. The prototypical tunneling structure, which is an essential element of nanostructures where electron tunneling is investigated, is a single barrier. The common model in these studies is a time-modulated potential that has a finite spatial profile. Standard electron transport through various types of time-oscillating potential regions has been studied previously. More pertinent to the work undertaken here is that of Buttiker and Landauer. They investigated the traversal time of particles interacting with a barrier with time-oscillating height.[4,5] Furthermore, Wagner[6] wrote a series of papers on photon-assisted transport through quantum wells and barriers with oscillating potentials. Exchange of photons between the oscillating potential and electrons transfers electrons to the sidebands with a finite probability. Wagner determined the transmission probabilities using transfer-matrix methods and discussed them as a function of the dimensionless parameter α which is the ratio of the amplitude of the time-oscillating potential to its modulation energy. There are other contributions to this field that are relevant to our work and these have been put together in Ref. 7. Recently, single-layer carbon crystals (graphene monolayer) were fabricated which has generated considerable interest in finding a material that can replace silicon in microelectronic devices. The idea of carbon-based nanoelectronics has been around since the discovery of carbon nanotubes. The recent fabrication of graphene monolayer has provided another avenue for carbon-based electronics. Devices based on photon-assisted electron tunneling require the consideration of electron transport in time-harmonic potentials. For graphene-based PAT devices it is essential to consider transport of charge carriers in graphene through time-harmonic potentials. To this end, we undertake the study presented here realizing that quasiparticles in graphene systems are quite different from the standard electrons that we encounter in conventional semiconductor-based heterostructures. At low energies, quasiparticles (electrons and holes) in graphene are described by the relativistic Dirac-type equation and possess charge-conjugation symmetry as a single equation describes both particles (electrons) and antiparticles (holes). This is due to the crystal structure of graphene which is a layer of carbon

atoms tightly packed in honeycomb lattice. It can be thought of as the superposition of two equivalent triangular sublattices conventionally called sublattices A and B. Quantum-mechanical hopping between these sublattices results in the formation of two cosinelike energy bands. Intersection of these bands near the edges of Brillouin zone (Dirac points) leads to the conical energy spectrum $E=\pm\hbar v_F k$ (with the effective Fermi speed $v_F=10^6$ m/s). Above zero energy, the charge carriers in these systems are electrons which are usually termed Dirac electrons. The two-dimensional (2D) Dirac-type spectrum was confirmed recently by cyclotron resonance measurements and also by angle-resolved photoelectron spectroscopy (ARPES) measurements.[8] Recent theoretical work on graphene multilayers has also shown the existence of Dirac electrons with a linear energy spectrum in monolayer graphene.[9] The Dirac equation implies that the quasiparticles in graphene are chiral. Tunneling through potential barriers in these systems is significantly different from systems where tunneling of standard electron occurs such as the two-dimensional electron-gas (2DEG) systems realized in semiconductor heterostructures. Chiral nature of particles in graphene results in quantum tunneling being highly anisotropic where relativistic effect such as perfect transmission through high and wide barriers can occur (Klein tunneling[10]).[11] This occurs due to conservation of chirality in interaction with the barrier. Electrons in graphene can propagate to hole states through a high barrier without any damping. The study of this effect is relevant to the development of future graphene-based devices. From a basic research point of view, graphene-based systems, due to their lower "light speed," can be quite useful for studying relativistic effects. Moreover, the role of chirality can be highlighted in electron transport in graphene. In graphene-based systems, electronic transport through barrier structures has been recently investigated.[11–19] In this work, we consider the transport of Dirac electrons in monolayer graphene through a square potential barrier harmonically oscillating in time. When standard electrons pass through a region which is subjected to time-harmonic potentials, electronic transitions from central band to sidebands occur. Here, when transmission of Dirac electrons is considered, we also find transitions from the central band to sidebands at energies $E\pm n\hbar\omega$ ($n=0,\pm1,\pm2,\ldots$) and determine the transmission probabilities for the sidebands. Moreover, we investigate how the transmission probabilities change as various parameters involved in the problem are varied with emphasis on the chiral nature of tunneling.

II. FORMULATION

We consider monolayer graphene sheet in the xy plane. The square potential barrier is taken to be in the x direction while particles are free in the y direction. The width of the barrier is a and the height of the barrier is oscillating sinusoidally around V with amplitude V_1 and frequency ω. Electrons with energy E are incident from one side of the barrier in graphene making an angle ϕ_0 with the x axis and leave the barrier with energy $E\pm n\hbar\omega$ ($n=0,\pm1,\ldots$) making angles ϕ_n after transmission and $\pi-\phi_n$ after reflection.

We consider the following Hamiltonian H describing the system:

$$H = H_0 + H_1, \tag{1}$$

where H_0 is the Hamiltonian for the static case where the barrier height is not changing with time and H_1 describes the harmonic time dependence of barrier height given by

$$H_0 = -i\hbar v_F \boldsymbol{\sigma}\cdot\boldsymbol{\nabla} + V, \tag{2}$$

$$H_1 = V_1\cos(\omega t). \tag{3}$$

V and V_1 are the static square potential barrier and the amplitude of the oscillating potential, respectively. Both V and V_1 are constants for $0\le x\le a$ with positive a and are zero elsewhere. $\boldsymbol{\sigma}=(\sigma_x,\sigma_y)$ are the Pauli matrices and v_F is the Fermi velocity.

Solutions of the Dirac equation in the absence of the oscillating potential, $H_0\Psi_0=E\Psi_0$, are given in Ref. 11 and can be used for constructing solutions to the time-dependent problem. For the tunneling problem, we consider the incoming electrons to be in plane wave states $\Psi_i(x,y,t)$ at energy E,

$$\Psi_i(x,y,t) = e^{ik_y y}\begin{pmatrix}1\\ s_0 e^{i\phi_0}\end{pmatrix}e^{ik_1^0 x}e^{-iEt/\hbar}, \tag{4}$$

where k_1^0 and k_y are the x and y components of the electron wave vector, respectively. $s_0=\mathrm{sgn}(E)$ and ϕ_0 is the angle that incident electrons make with the x axis.

Reflected and transmitted waves have components at all energies $E\pm l\hbar\omega$ ($l=0,\pm1,\ldots$) since the oscillating potential barrier can give and take energy away from electrons in units of $\hbar\omega$. This change in energy causes only the x component of momentum to change. Hence, wave functions $\Psi_r(x,y,t)$ for reflected and $\Psi_t(x,y,t)$ for transmitted electrons, respectively, are

$$\Psi_r(x,y,t) = e^{ik_y y}\sum_{l=-\infty}^{l=\infty} r_l\begin{pmatrix}1\\ -s_l e^{-i\phi_l}\end{pmatrix}e^{-ik_1^l x}e^{-i(E+l\hbar\omega)t/\hbar} \tag{5}$$

and

$$\Psi_t(x,y,t) = e^{ik_y y}\sum_{l=-\infty}^{l=\infty} t_l\begin{pmatrix}1\\ s_l e^{i\phi_l}\end{pmatrix}e^{ik_1^l x}e^{-i(E+l\hbar\omega)t/\hbar}, \tag{6}$$

where

$$k_1^l = \sqrt{\left(\frac{E+l\hbar\omega}{\hbar v_f}\right)^2 - k_y^2},$$

$$\phi_l = \tan^{-1}(k_y/k_1^l),$$

$$s_l = \mathrm{sgn}(E+l\hbar\omega).$$

In the barrier region, where H_1 is nonzero, the eigenfunctions $\Psi_b(x,y,t)$ of H can be expressed in terms of the eigenfunctions $\Psi_0(x,y)$ of H_0 as[3]

$$\Psi_b(x,y,t) = \Psi_0(x,y) \sum_{n=-\infty}^{n=\infty} J_n\left(\frac{V_1}{\hbar\omega}\right) e^{-in\omega t - iEt/\hbar},$$

where $J_n(\frac{V_1}{\hbar\omega})$ is the nth-order Bessel function. A linear combination of wave functions at energies $E+l\hbar\omega$ ($l=0,\pm 1,\ldots$) has to be taken. Hence,

$$\Psi_b(x,y,t) = e^{ik_y y} \sum_{l=-\infty}^{l=\infty} \left[B_l \begin{pmatrix} 1 \\ s_l' e^{i\phi_l'} \end{pmatrix} e^{ik_2^l x} + C_l \begin{pmatrix} 1 \\ -s_l' e^{-i\phi_l'} \end{pmatrix} e^{-ik_2^l x} \right] \times \sum_{n=-\infty}^{n=\infty} J_n\left(\frac{V_1}{\hbar\omega}\right) e^{-i(n+l)\omega t - iEt/\hbar}, \quad (7)$$

where

$$k_2^l = \sqrt{\left(\frac{E - V + l\hbar\omega}{\hbar v_f}\right)^2 - k_y^2},$$

$$\phi_l' = \tan^{-1}(k_y/k_2^l),$$

$$s_l' = \mathrm{sgn}(E + l\hbar\omega - V).$$

The wave functions given in Eqs. (4)–(7) have to be continuous at the boundary. Applying this condition at $x=0$ and a, i.e., $\Psi_i(0,y,t)+\Psi_r(0,y,t)=\Psi_b(0,y,t)$ and $\Psi_t(a,y,t)=\Psi_b(a,y,t)$ and realizing that $\{e^{in\omega t}\}$ are orthogonal, we obtain the following set of simultaneous equations:

$$A_n + r_n = \sum_{l=-\infty}^{l=\infty} [B_l + C_l] J_{n-l}\left(\frac{V_1}{\hbar\omega}\right), \quad (8)$$

$$A_n e^{i\phi_n} - r_n e^{-i\phi_n} = s_n \sum_{l=-\infty}^{l=\infty} [B_l e^{i\phi_l'} - C_l e^{-i\phi_l'}] s_l' J_{n-l}\left(\frac{V_1}{\hbar\omega}\right). \quad (9)$$

Here $A_n=\delta_{n,0}$;

$$t_n e^{ik_1^n a} = \sum_{l=-\infty}^{l=\infty} [B_l e^{ik_2^l a} + C_l e^{-ik_2^l a}] J_{n-l}\left(\frac{V_1}{\hbar\omega}\right), \quad (10)$$

$$t_n e^{i\phi_n} e^{ik_1^n a} = s_n \sum_{l=-\infty}^{l=\infty} [B_l e^{i\phi_l'} e^{ik_2^l a} - C_l e^{-i\phi_l'} e^{-ik_2^l a}] s_l' J_{n-l}\left(\frac{V_1}{\hbar\omega}\right). \quad (11)$$

The above set has infinite number of coupled equations and contains infinite number of unknowns (n,l goes from $-\infty$ to ∞). This linear system of equations cannot be analytically solved. Nevertheless, the infinite series in these coupled equations can be truncated and a finite number of terms starting from $-N$ up to N, where $N > \frac{V_1}{\hbar\omega}$, retained if we note that the coupling strength is determined by the quantity $\frac{V_1}{\hbar\omega}$ through Bessel functions $J_n(\frac{V_1}{\hbar\omega})$, that are negligible for n order higher than $V_1/\hbar\omega$. Equations (8)–(11) are numerically solved for t_n. The transmission probability for the nth sideband T_n, for which k_1^n is real and corresponds to propagating waves, is obtained from

$$T_n = \frac{\cos\phi_n}{\cos\phi_0} |t_n|^2, \quad (12)$$

whereas imaginary k_1^n corresponds to evanescent waves that carry no particle current with the result $T_n=0$. k_1^n can be real or imaginary depending on the particular values of the following parameters: incident energy E, oscillation frequency ω, and incident angle ϕ_0. The numerical results obtained are discussed in Sec. III. Furthermore, analytical results are obtained if we consider small values of $\alpha=\frac{V_1}{\hbar\omega}$ and include only the first two sidebands at energies $E\pm\hbar\omega$ along with the central band at energy E. Moreover, we have to invoke the condition $\hbar\omega < E$ such that $\mathrm{sgn}(E\pm\hbar\omega)=+1$ and $\hbar\omega < |E-V|$ such that $\mathrm{sgn}(E-V\pm\hbar\omega)=-1$ for $E<V$. Hence, we are able to truncate the sums in Eqs. (8)–(11) retaining only the terms corresponding to the central band and first sidebands and obtain analytical results for central band and first sidebands t_0 and $t_{\pm 1}$ as follows:

$$t_0 = \frac{e^{-ik_1^0 a} \cos\theta_0 \cos\phi_0}{\cos\theta_0 \cos\phi_0 \cos[k_2^0 a] + i \sin[k_2^0 a](1 + \sin\theta_0 \sin\phi_0)},$$

$$t_n = \frac{1}{2}\frac{J_n(\alpha)}{J_0(\alpha)} \frac{t_{s0} t_{sn}}{\cos\phi_n} [\Gamma_n^+ + \Gamma_n^- e^{i(\phi_0+\phi_n)} + \Delta_n (e^{i\phi_0} + e^{i\phi n})] \times e^{i(\phi_n + k_1^0 a)},$$

where $n=\pm 1$. t_{s0} and t_{sn} are transmission amplitudes for the static barrier at energy E and $E+n\hbar\omega$ and

$$\Gamma_n^{\pm} = \Lambda_n^{\pm} - \Lambda_0^{\pm},$$

$$\Lambda_n^{\pm} = \cos[k_2^n a \pm \theta_n]/\cos\theta_n,$$

$$\Delta_n = \Omega_n - \Omega_0,$$

$$\Omega_n = i \sin[k_2^n a]/\cos\theta_n.$$

In the high-barrier limit, $|V| \gg E$ with the result $\theta_0, \theta_n \to 0$. We obtain expressions for transmission probabilities for the central band and sidebands. For the central band

$$T_0 \approx \frac{\cos^2\phi_0}{1 - \cos^2[k_2^0 a]\sin^2\phi_0} = T_{s0}, \quad (13)$$

where T_{s0} denotes the transmission probability at incident energy E and incident angle ϕ_0 in the case of the static barrier. This is the result obtained as Eq. (4) in Ref. 11. For sidebands, we obtain

$$\Lambda_n^{\pm} = \cos[k_2^n a] \Rightarrow \Gamma_n^{\pm} = -2 \sin[(k_2^n + k_2^0)a/2]\sin[(k_2^n - k_2^0)a/2],$$

$$\Omega_n = i \sin[k_2^n a] \Rightarrow \Delta_n = 2i \cos[(k_2^n + k_2^0)a/2]\sin[(k_2^n - k_2^0)a/2],$$

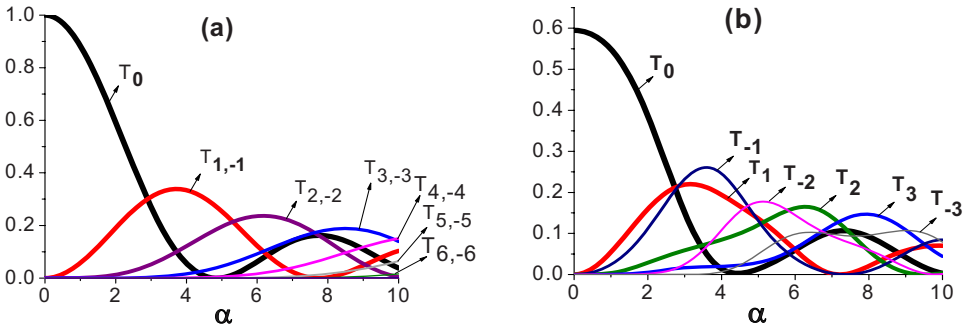

FIG. 1. (Color online) Transmission probabilities for central band and first few sidebands as a function of $\alpha \equiv V_1/\hbar\omega$ (a) for normally incident electrons and (b) for incidence angle of 30°.

$$t_n = 2i\frac{J_n(\alpha)}{J_0(\alpha)}\frac{t_{s0}t_{sn}}{\cos\phi_n}\sin[(k_2^n - k_2^0)a/2](\cos[(k_2^n + k_2^0)a/2] \times \cos[(\phi_n - \phi_0)/2] + i\sin[(k_2^n + k_2^0)a/2] \times \cos[(\phi_n + \phi_0)/2])e^{i[k_1^0 a + (\phi_0 - \phi_n)/2]}.$$

The transmission probability for the sidebands is given by

$$T_n = \frac{\cos(\phi_n)}{\cos(\phi_0)}|t_n|^2 = T_{s0}T_{sn}\left[2\frac{J_n(\alpha)}{J_0(\alpha)}\right]^2 \times \frac{\sin^2[(k_2^n - k_2^0)a/2]}{\cos\phi_n\cos\phi_0}\{\cos^2[(k_2^n + k_2^0)a/2]\cos^2[(\phi_n - \phi_0)/2] + \sin^2[(k_2^n + k_2^0)a/2]\cos^2[(\phi_n + \phi_0)/2]\},$$

where $\hbar\omega < E\cos\phi_0$; otherwise, $T_{-1}=0$. $T_{sn}=|t_{sn}|^2$ is the transmission probability of electrons at energy $E+n\hbar\omega$ and incident angle ϕ_n for the static barrier. We can also write the above expression as

$$T_n = T_{s0}T_{sn}\left[2\frac{J_n(\alpha)}{J_0(\alpha)}\right]^2\frac{\sin^2[(k_2^n - k_2^0)a/2]}{\cos\phi_n\cos\phi_0} \times \{\sin\phi_0\sin\phi_1\cos^2[(k_2^0 + k_2^1)a/2] + \cos^2[(\phi_0 + \phi_1)/2]\}. \quad (14)$$

At normal incidence,

$$T_{\pm 1} = \left(2\frac{J_{\pm 1}(\alpha)}{J_0(\alpha)}\right)^2\sin^2[(k_2^0 - k_2^{\pm 1})a/2]$$

and if $\hbar\omega < |E-V|$ we can write

$$k_2^0 - k_2^{\pm 1} = |E-V|/\hbar v_F - |E - V \pm \hbar\omega|/\hbar v_F = \pm\omega/v_F$$

with the result

$$T_{\pm 1} = \left(2\frac{J_{\pm 1}(\alpha)}{J_0(\alpha)}\right)^2\sin^2\left[\frac{\omega a}{2v_F}\right] = \left(2\frac{J_{\pm 1}(\alpha)}{J_0(\alpha)}\right)^2\sin^2[\omega\tau/2],$$

where $\tau \equiv a/v_F$ is the time taken by a normally incident electron to cross the barrier *without multiple reflections* inside it. From the above expression, we note that $T_1 = T_{-1}$. For small α, $J_{\pm 1}(\alpha) \approx \pm\alpha/2$; $J_0(\alpha) \approx 1$ and $\sin[\omega\tau/2] \approx \omega\tau/2$ when $\omega\tau$ is small, corresponding to low-frequency limit where frequency is smaller than the reciprocal of the traversal time. Using these results we obtain

$$T_{\pm 1} \approx \left(\frac{V_1}{2\hbar}\tau\right)^2.$$

The above result can be compared with Eq. (8) in Ref. 4, where the transmission probability through a time-modulated barrier for the first sidebands was determined. The factor T, the transmission probability of the central band, is not unity and hence it appears there whereas $T_{s0}=T_{sn}=1$, at normal incidence, in our case.

III. RESULTS AND DISCUSSIONS

The results for the transmission of Dirac electrons in graphene are now presented. The following parameters were used. The Fermi wavelength of the incident electron is taken to be $\lambda = 50$ nm, the barrier oscillation frequency is $\omega = 5 \times 10^{12}$ Hz, the barrier width is $a = 100$ nm, and the barrier height is $V = 200$ meV. The dependence of transmission probabilities on $\alpha = V_1/\hbar\omega$ for normally incident electrons and for those arriving at an incident angle of 30° is shown in Figs. 1(a) and 1(b), respectively. For normal incidence, the angular dependence of the transmission probability for the nth sideband is independent of the sign of n; $T_{+n}=T_{-n}$ for real $k_1^{-|n|}$. But this does not hold for incidence other than normal. We also find that the quantity α is very significant in determining the relative transmission probabilities of various sidebands as shown in the figure. This implies that by adjusting the value of α we can increase transmission through a particular sideband. It is seen that the central band dominates the transmission at all incident angles for small values of α, whereas contributions from higher and lower sidebands increase as α becomes larger. This is plausible because for lower values of α the oscillating barrier can be treated as a static one since we are keeping ω fixed and changing V_1 with the result that α is proportional to V_1 in these figures. Moreover, the total transmission probability through the central band as well as the sidebands is unity. Hence, perfect transmission for the oscillating barrier at normal incidence which was earlier observed for the static barrier is present.[11] This is due to chiral nature of the particles which results in perfect transmission (Klein tunneling).

In Fig. 2(a) we present the angular dependence of the transmission probability for the central band T_0 for various values of $\alpha = V_1/\hbar\omega$. The transmission probability for the static barrier is also shown in the figure as it corresponds to $\alpha = 0$. The transmission probability T for the static barrier was previously obtained in Ref. 11. We find resonant trans-

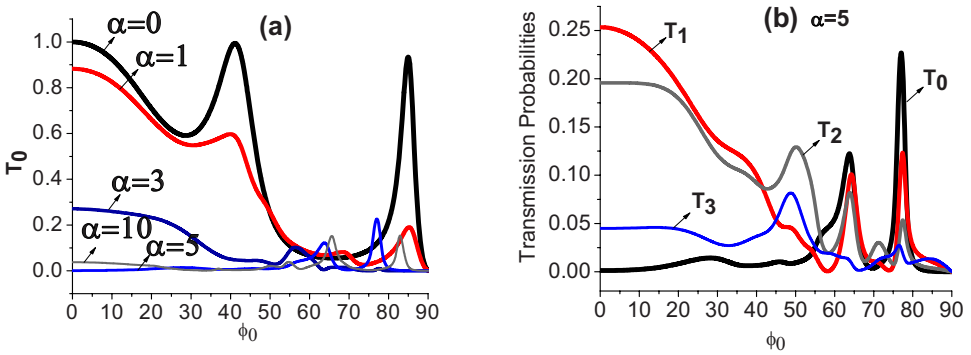

FIG. 2. (Color online) Transmission probability as a function of the incident angle (a) for central band for different values of α and (b) for first three upper sidebands and central band for $\alpha=5$.

mission through the oscillating barrier but unlike the static barrier we do not find perfect transmission for any incident angle. Realize that for the static barrier there is perfect transmission for certain values of the incident angle. This is to be expected as the probabilities are now spread over the central band and sidebands. In addition, the maximum transmission through the oscillating barrier depends on the value of α.

Figure 2(b) shows the transmission probabilities for the central band along with the first few sidebands as a function of the incident angle for $\alpha=V_1/\hbar\omega=5$. In this figure, we show how the incident-particle flux is distributed in the sidebands (through the respective transmission probabilities) as the incident angle is varied. Note that the propagation angle for nth sideband is ϕ_n which is not the same as the incident angle ϕ_0. For this particular value of α, the transmission probability in the central band is very small for normal and close to normal incidence. For higher sidebands, more and more peaks in transmission probabilities occur. In the static case, the peaks in the transmission probability of the central band (there are no sidebands there) correspond to perfect transmission and the incident angles at which these occur can be obtained from the resonance condition $k_2^l=\frac{p\pi}{a}$ (p is an integer) through Eq. (13) and Ref. 11. For the time-dependent situation investigated here, it is not easy to determine the positions of the peaks as the analytical expression is more complicated. Nevertheless, we can understand how and where they occur by examining Eq. (14), albeit for small α where analytical results can be obtained but essential physics remains unchanged. We observe that the transmission probability T_n given by Eq. (14) depends most strongly on the prefactor $T_{s0}T_{sn}$ for the parameters considered here. The peaks correspond to the peak values of $T_{s0}T_{sn}$. Furthermore, the same behavior is seen for the static case as the transmission at higher incident energy there corresponds to transmission in the sidebands here. At these higher energies, the x component of momentum in the barrier region satisfies the resonance condition a greater number of times as the incident angle is varied; thus, larger number of peaks is obtained.

We note that the absence of any potential gradient along the y direction results in the conservation of the y component of momentum. Therefore, change in energy that an electron experiences due to exchange of modulation quanta with the oscillating barrier brings about corresponding changes only in the x component of the electron's momentum. For nonzero k_y, energy exchanges can make x component of momentum imaginary inside or/and outside the barrier region that corresponds to unavailability of any energy state in the relevant region(s). If energy $E+l\hbar\omega$ in the lth sideband is such that $|E+l\hbar\omega|<\hbar v_F k_y$, there are no propagating states available outside the barrier since k_1^l becomes imaginary. At the same energy when particles have states available inside the barrier, it can be localized if it is transferred to these states after losing energy through interaction with the oscillating barrier. In this situation, the particles are confined across the barrier while they are free to propagate along the barrier until one or more quantum of energy is absorbed, allowing transition to a higher sideband with states aligned in energy outside the barrier leading to eventual escape from the barrier region. For a graphene quantum well, confined electron states which arise due to the suppression of electron-hole conversion at the barrier have been discussed in Ref. 15.

For electron energy such that $|E+l\hbar\omega-V|<\hbar v_F k_y$, there are no propagating states available inside the barrier since k_2^l becomes imaginary. Furthermore, for the energy at which electronic states outside the barrier match the hole states inside it, electronic transmission is governed by Klein tunnel-

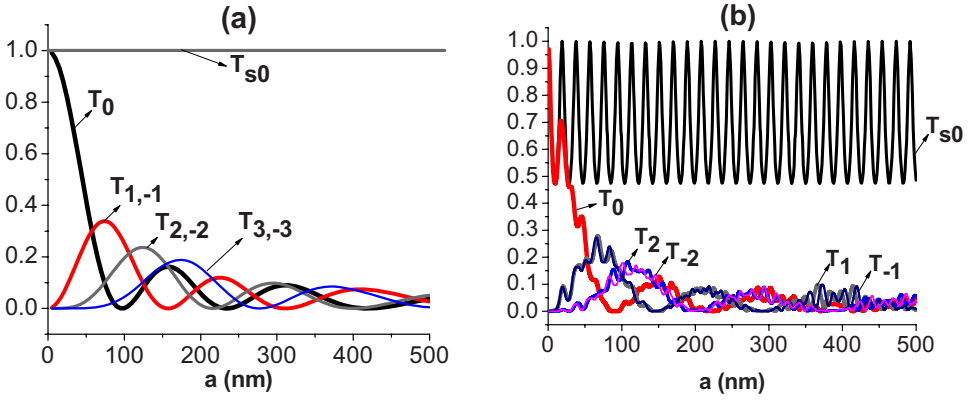

FIG. 3. (Color online) Transmission probability of electrons for central band and first few sidebands for $\alpha=5$ along with that for static barrier as a function of the barrier width (a) for normal incidence and (b) for angle of incidence of 30°.

ing while unavailability of hole states inside the barrier results in ordinary tunneling.

In Fig. 3(a) we present the transmission probability as a function of barrier width a for normal incidence at $\alpha=5$. For the static barrier there is a perfect transmission as can be seen in Fig. 3(a) where T represents the transmission probability for the static barrier, whereas the transmission probability for the central band in the oscillating barrier decreases for smaller values of the barrier width and shows oscillatory but damped behavior for larger barrier width. The transmission probability for the other sidebands increases initially from zero but then oscillates with damped amplitude. We also observe that the contribution in transmission of the higher sidebands rises as the barrier width increases. This occurs due to larger time available for the electron to interact with the oscillating potential as it traverses the barrier. In addition, we find that for normal incidence in the oscillating barrier $T_{+n}=T_{-n}$ for real $k_1^{-|n|}$. Moreover, the total transmission probability through the central band as well as the sidebands is unity. These results imply that perfect transmission at normal incidence is independent of the barrier width which is yet another manifestation of Klein tunneling.

In Fig. 3(b), the transmission probability as a function of barrier width a when the incident angle is 30° is shown. The transmission probability represented by T for the static barrier now oscillates as a function of the barrier width, whereas transmission probabilities for the central band and sidebands in the oscillating barrier show behavior close to that obtained for normal incidence.

A comparison between analytical result obtained in Eq. (14) and numerical results is presented in Fig. 4 for $\alpha=0.5$. Transmission probabilities $T_{\pm 1}$ of first sidebands are plotted against incident angle ϕ_0. Inset shows plot of T_{-1} versus ϕ_0. It is observed that transmission probabilities determined numerically exhibit the same behavior as obtained analytically.

To summarize, we have considered the tunneling of chiral massless electrons in monolayer graphene through a barrier that is oscillating harmonically in time. We have determined how the transmission probability for the central band and sidebands depends on the incident angle of the particles, the width of the barrier, the height, and frequency with which it oscillates. Due to the chiral nature of the particles in graphene, tunneling is highly anisotropic with peculiar behavior at normal and close to normal incidence (Klein tunneling). We find, for normal incidence, perfect transmission in monolayer graphene. Klein tunneling that was observed for the static barrier is found to persist for the oscillating barrier.

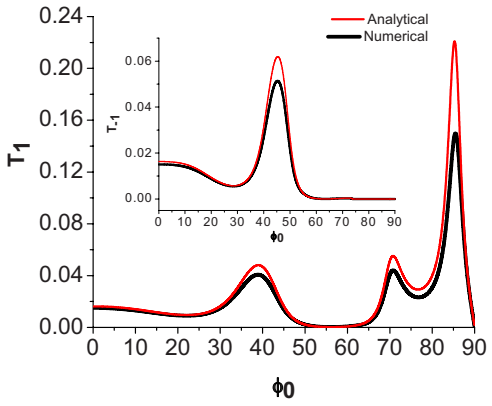

FIG. 4. (Color online) Comparison of analytical and numerical results. Transmission probability of first sidebands as a function of incident angle for $\alpha=0.5$.

ACKNOWLEDGMENTS

One of us (K.S.) would like to acknowledge the support of the Pakistan Science Foundation (PSF) through Project No. C-QU/Phys (129).

*Corresponding author; ksabeeh@qau.edu.pk; kashifsabeeh@hotmail.com

[1] G. Platero and R. Aguado, Phys. Rep. **395**, 1 (2004).
[2] A. H. Dayem and R. J. Martin, Phys. Rev. Lett. **8**, 246 (1962).
[3] P. K. Tien and J. P. Gordon, Phys. Rev. **129**, 647 (1963).
[4] M. Buttiker and R. Landauer, Phys. Rev. Lett. **49**, 1739 (1982).
[5] M. Buttiker, Phys. Rev. B **27**, 6178 (1983); M. Buttiker and R. Landauer, Phys. Scr. **32**, 429 (1985).
[6] M. Wagner, Phys. Rev. B **49**, 16544 (1994); Phys. Rev. A **51**, 798 (1995); Phys. Rev. Lett. **76**, 4010 (1996); Phys. Status Solidi B **204**, 328 (1997); M. Wagner and W. Zwerger, Phys. Rev. B **55**, R10217 (1997); M. Wagner, *ibid.* **57**, 11899 (1998).
[7] C. S. Tang and C. S. Chu, Phys. Rev. B **53**, 4838 (1996); C. S. Chu and H. C. Liang, Chin. J. Phys. **37**, 411 (1999); P. F. Bagwell and R. K. Lake, Phys. Rev. B **46**, 15329 (1992); W. Li and L. E. Reichl, *ibid.* **60**, 15732 (1999); C.-L. Ho and C.-C. Lee, Phys. Rev. A **71**, 012102 (2005); Q. F. Sun, J. Wang, and T. H. Lin, Phys. Rev. B **58**, 2008 (1998); X. G. Zhao, G. A. Georgakis, and Q. Niu, *ibid.* **56**, 3976 (1997); J. D. White and M. Wagner, *ibid.* **48**, 2799 (1993); C. S. Kim and A. M. Satanin, *ibid.* **58**, 15389 (1998); M. Y. Azbel, *ibid.* **43**, 6847 (1991); M. Covington, M. W. Keller, R. L. Kautz, and J. M. Martinis, Phys. Rev. Lett. **84**, 5192 (2000); M. Sweeny and J. Xu, IEEE J. Quantum Electron. **25**, 885 (1989).
[8] R. S. Deacon, K.-C. Chuang, R. J. Nicholas, K. S. Novoselov, and A. K. Geim, Phys. Rev. B **76**, 081406(R) (2007); S. Y. Zhou, G.-H. Gweon, J. Graf, A. V. Fedorov, C. D. Spataru, R. D. Diehl, Y. Kopelevich, D. H. Lee, S. G. Louie, and A. Lanzara, Nat. Phys. **2**, 595 (2006).
[9] B. Partoens and F. M. Peeters, Phys. Rev. B **75**, 193402 (2007).
[10] O. Klein, Z. Phys. **53**, 157 (1929).
[11] M. I. Katsnelson, K. S. Novoselov, and A. K. Geim, Nat. Phys. **2**, 620 (2006).
[12] H. B. Heersche, P. Jarillo-Herrero, J. B. Oostinga, L. M. K. Vandersypen, and A. F. Marpurgo, Nature (London) **446**, 56 (2007).
[13] D. Dragoman and M. Dragoman, Appl. Phys. Lett. **90**, 143111 (2007).

[14] B. Trauzettel, Ya. M. Blanter, and A. F. Morpurgo, Phys. Rev. B **75**, 035305 (2007).
[15] J. M. Pereira, V. Mlinar, F. M. Peeters, and P. Vasilopoulos, Phys. Rev. B **74**, 045424 (2006).
[16] V. V. Cheianov and V. I. Falko, Phys. Rev. B **74**, 041403(R) (2006).
[17] J. Milton Pereira, Jr., P. Vasilopoulos, and F. M. Peeters, Appl. Phys. Lett. **90**, 132122 (2007).
[18] Michaël Barbier, F. M. Peeters, P. Vasilopoulos and J. Milton Pereira, Phys. Rev. B **77**, 115446 (2008).
[19] A. Matulis and F. M. Peeters, Phys. Rev. B **77**, 115423 (2008).